GEOLOGICAL SURVEY OF CANADA
OPEN FILE 7593

Time-domain electromagnetic data for the Spiritwood valley aquifer, Manitoba

G.A. Oldenborger and K. Brewer

2014

Natural Resources
Canada

Ressources naturelles
Canada

Canada

GEOLOGICAL SURVEY OF CANADA
OPEN FILE 7593

Time-domain electromagnetic data for the Spiritwood valley aquifer, Manitoba

G.A. Oldenborger and K. Brewer

2014

Recommended citation
Oldenborger, G.A. and Brewer, K., 2014. Time-domain electromagnetic data for the Spiritwood valley aquifer, Manitoba; Geological Survey of Canada, Open File 7593. doi:10.4095/293700

Publications in this series have not been edited; they are released as submitted by the author.

ABSTRACT

This Open File reports on recent time-domain electromagnetic geophysical data collected and processed by the Geological Survey of Canada as part of the Aquifer Assessment and Support to Mapping project within the Groundwater Geoscience Program. A 1062 km^2 area of the Spiritwood valley aquifer in southern Manitoba has been developed as a site for testing the application of airborne electromagnetics and other surface and downhole geophysical methods for regional mapping and characterization of buried valley aquifers in Canada. In November of 2013, time-domain electromagnetic soundings were performed at selected sites to better constrain the airborne results. One-dimensional modelling and inversion of the data show marked variability in the data and the resistivity models between different geological settings. In particular, depth to bedrock is clearly resolved in the models and the incised buried valley interpreted from the regional airborne survey is associated with a relatively strong resistive anomaly indicative of coarser grained material or a high-potential aquifer.

TABLE OF CONTENTS

INTRODUCTION

Buried valleys occur beneath the glaciated terrains of Canada and other countries. When filled with coarse-grained permeable sediments, these valleys represent potential sources of groundwater. Productive buried valley aquifers are common in Canada, yet knowledge of their distribution and groundwater resource potential is inadequate (Russell et al. 2004; Betcher et al. 2005; van der Kamp and Maathius 2012). Systematic mapping and resource evaluation of buried valleys is hindered by complicated network geometries, the lack of surface expression, and longitudinal and cross-sectional variability. Buried valley systems may represent preferential flow paths that may have significant influence on regional groundwater flow regimes, but may go unmapped or uncharacterized in traditional hydrogeological studies (e.g., Shaver and Pusc 1992) especially in the absence of regionally extensive or continuous data.

As part of a multi-disciplinary effort, the Geological Survey of Canada (GSC) has been investigating the applicability of airborne electromagnetics (AEM) for mapping and characterization of buried valley aquifer systems (Oldenborger et al., 2013a; 2013b; Pugin et al., 2014; Sapia et al., 2012; Sapia et al., 2014a; 2014b). In particular, a suite of data has been collected for the Spiritwood valley aquifer in southern Manitoba including a 1062 km^2 AeroTEM III survey (Oldenborger, 2010a; 2010b; Oldenborger et al., 2010), electrical resistivity data (Oldenborger et al., 2013), seismic reflection data (Pugin et al., 2011), borehole data (Crow et al., 2012a; 2012b), several lines of VTEM data (Legault et al., 2012), and a small block of fixed-wing TEMPEST and MULTIPULSE data (J. Lemieux, CGG, personal communication).

AEM data provide rapid, high-density data acquisition at regional scales not achievable by ground surveys, whereas the ground geophysical and geological data are used to corroborate and evaluate the AEM results and to better understand the AEM response. Electrical resistivity models derived from the AeroTEM data over the Spiritwood valley give a sense of the full buried valley geometry, the variability of valley orientation and fill material, the complexity of multiple valley relations and stratigraphic nesting of valleys (Oldenborger et al., 2013). Valley features interpreted from the resistivity models are in agreement with valley features interpreted from the seismic reflection and electrical resistivity surveys. However, models derived from the AeroTEM data do not discriminate the variability in the near-surface or in the surficial till package that is observed in the higher resolution geophysical data, although there is some indication of near-surface heterogeneity. Furthermore, discrimination of the electrical properties of the different sedimentary units (i.e., till, sand/gravel, bedrock) is difficult using the AEM data alone (Sapia et al., 2012; 2014a). Limitations arise from the finite bandwidth of the AEM system, possible AEM system timing errors, errors introduced during data processing and errors in the modelling of the electromagnetic response.

Although other types of ground-based information contribute to understanding these limitations, much of the comparison is necessarily qualitative or structural in nature. Ground-based time-domain electromagnetic (TEM) data provide an opportunity for quantitative comparison or calibration of AEM data (Foged et al., 2013; Podgorski et al., 2013). To this end, the GSC initiated collection of TEM soundings at selected Spiritwood sites indicative of certain nominal target types such as buried valley, till or bedrock as interpreted from the regional AEM results. Sites were also selected to further leverage complementary seismic and electrical surveys. This Open File details collection, processing and inversion of these TEM data to generate one-dimensional (1D) resistivity models at the sounding sites.

GEOGRAPHICAL CONTEXT

The Spiritwood valley is buried bedrock valley in southern Manitoba that runs approximately northwest-southeast near the towns of Killarney and Cartwright and extends 500 km from Manitoba, across North Dakota and into South Dakota (Bluemle, 1984; Winter et al. 1984). The valley has little or no surface topographic expression and was identified and geographically constrained as a municipal and rural source of groundwater primarily based on water well information (Wiecek 2009).

In North Dakota the valley has been defined by a series of borehole transects to be up to 15–20 km wide and 100–150 m deep (Randich and Kuzniar, 1984). The underlying bedrock is a fractured siliceous shale from the Odanah Member of the Pierre Formation. The stratigraphy within the valley is variable and includes a basal sand and gravel, overlain by a series of undefined clay/silt till units locally interstratified with sands of variable thickness and extent. The basal sand and gravel is not observed throughout the valley, but together with the inter-till sands, it represents potential aquifer material.

DATA ACQUISITION

The TEM data presented in this Open File were collected from November 11–14, 2013. Sounding sites were selected to represent target features observed in the AeroTEM survey. Where possible sites were also located along seismic and/or electrical resistivity sections (Table 1, Figure 1). Site conditions were entirely farmland that had been cropped or plowed that autumn and the ground surface was frozen.

Table 1. TEM sounding locations and nominal target type (NAD83, UTM Zone 14N).

Section	Site	Easting (m)	Northing (m)	Target Type
S2007	1	444736	5467286	Buried Valley
S2007	2	443872	5467183	Till
S2007	3	448192	5467022	Bedrock
S3	1	464077	5449532	Buried Valley
S3	2	466842	5450902	Bedrock
S3	3	464015	5447803	Till
S3	4	462341	5448873	Shallow Valley
S2	1	476056	5438902	Buried Valley
S2	2	477656	5439293	Till

Data were collected with a digital 20-gate ProTEM-D receiver (SN 959704), a TEM47 transmitter (SN 031892), a TEM57-MK2 transmitter (SN 10057) and a high-frequency (HF) receiver coil (SN 0301) all manufactured by Geonics Ltd. In all cases, the transmitter utilized an 80 m × 80 m single-coil rectangular loop comprised of AWG 12 stranded Copper wire with a resistance of approximately 2 Ω. Dual transmitters were utilized to take advantage of both the high frequency and early-time capability of the TEM47 and the higher current and lower frequency of the TEM57. We thereby ensure near-surface resolution, while at the same time increasing depth penetration to recover depth to bedrock under the buried valleys.

All soundings were acquired in a central-loop configuration using base frequencies of 285 Hz (u), 75 Hz (v) and 30 Hz (H) with the TEM47, and 30 Hz (H) and 7.5 Hz (M) with the TEM57.

Data were collected as 3 records per frequency and each record was stacked according to the integration times of 4 s (u), 8 s (v), 30 s (H) and 60 s (M). Gain was set variably in order to keep ambient noise (transmitter-off) below +/-5 nV/m^2 in the last 5 time gates at any frequency, and to avoid any early-time saturation of the signal (transmitter-on). In most cases, an ambient noise record was collected for each frequency of acquisition using the same gain parameters as the data. The raw data are provided in the Appendix.

PROCESSING AND INVERSION

Data processing involves characterization of noise, record selection, and removal of outliers. Acquiring 3 stacked records per frequency allows for rejection of transient noise. For each frequency, a single data record of induced voltage (mV) is computed on a gate-by-gate basis as the median value for each of the 3 records. In most cases, the records are highly repeatable with medians indistinguishable from the means. Not surprisingly, the data are generally less repeatable at later times and for lower frequency with the same transmitter, and repeatability errors are usually larger than the ambient noise level but of the same order of magnitude. The observed noise levels are certainly not constant either in terms of percentage or absolute value and this must be reflected in the inversion by choice of an appropriate noise model.

Although noise levels could be assigned on a frequency-by-frequency and gate-by-gate basis using the observed repeatability errors and ambient noise levels, it is perhaps more representative to apply a generalized noise model – this is the approach taken here. We adopt a noise model of the form $p = a \, e^{b \cdot g} + c$ where p is the noise level (%), g is the integer time gate, and a, b and c are empirically fit constants based on the raw data. The median soundings and noise models are provided in the Appendix.

Given a data sounding and a noise model, it is important to remove outliers or overly noisy data and deal with inconsistent data before inversion. For TEM data collected with variable gain, moment, and gate times, identification of errors or noise is aided by normalization. We first normalize the received voltage to a transmitter of unit area, current, and gain (V/Am^2). Such a normalization is equivalent to transformation of the loop voltage to the time rate of change of the magnetic field (T/s). At this point, some random noise at late time is easily identified by erratic spikes, oscillations or sign reversals; these data are removed on a case-by-case basis. More systematic noise can be present due to coupling with cultural features such as power lines or grounded fences (Danielsen et al., 2003). The Spiritwood TEM data do not appear to be contaminated by capacitive coupling. Galvanic coupling is difficult to identify for isolated soundings, but would result in anomalously low resistivity after inversion.

Another form of systemic noise that is prevalent in multi-frequency data is a transmitter run-on effect. Given the finite signal period, there may be situations wherein the voltage induced in the receiver due to the transmitter turn-on has not fully decayed before turn-off and initiation of the first off-time measurement gate. In this situation, a sounding will have components attributable to both the transmitter turn-on and turn-off that are of opposite sign resulting in a reduction of the total induced voltage at the receiver. In relatively conductive environments with slow current decay, it is also possible for signal associated with the transmitter turn-off to extend into the next off-time measurement period (e.g., Haber et al., 2007). These sorts of effects are more easily identified after transformation to late-time apparent resistivity which further normalizes for measurement time (e.g., Spies and Eggers, 1986).

We observe that the last 3–5 time gates at any particular frequency are systematically inconsistent with the contemporaneous gates of the next lower frequency. In general, we remove the last 4 gates at each frequency. Under the apparent resistivity transform, there is also an apparent inconsistency between the 30 Hz TEM47 data and the 30 Hz TEM57 data. At least some of this inconsistency (or nearly all of it) can be attributed to the differences in the duration of the turn-off ramp for the different transmitters: 4.4 μs for the TEM47 and ~50 μs for the TEM57. The apparent resistivity transform assumes a perfect step-off meaning that the transformation is not equivalent for the different transmitters. Furthermore, ProTEM gate times are relative to the end of the turn-off ramp and are thus out-of-sync for the different transmitters, an effect that will be more pronounced for early times. In general, we remove the 30 Hz TEM57 data entirely in addition to the first few gates of the 7.5 Hz TEM57 data prior to inversion. Tests including the 30 Hz TEM57 data did not yield significantly different inverse models.

Once the data have been edited for noise, they are merged into a single multi-frequency sounding at each site where each frequency is assigned a unique ramp turn-off time. Correctly establishing the ramp turn-off time is critical for accurate model recovery, particularly in the near surface. Each sounding is inverted using EM1DTM (Farquharson and Oldenburg, 1993). EM1DTM is based on an over-determined, least-squares one-dimensional inversion algorithm that operates on a layered-Earth parameterization. For all sites, we use a 38-layer model with layer thickness increasing logarithmically from 3 m at the surface. The starting and reference models are homogeneous with a resistivity of 5 Ωm. The inversion incorporates variable noise weighting and attempts to fit the data to a level commensurate with the noise. In most cases, the inversions converge to χ^2 values greater than unity indicating that our noise estimates may be too small. However, RMS misfit is typically good with most of the misfit attributable to late times which suggests that our noise model is appropriate in relative terms if not in absolute values.

The 1D resistivity models provided in the Appendix are the result of iterative processing, filtering and multiple inversions of the data. We include both the L_2 (smooth) model in addition to the L_1 (blocky) model obtained via iteratively re-weighted least-squares (Farquharson and Oldenburg, 1998). Based on the L_2 models, we estimate the model reliability using the depth of investigation (DOI) concept applied to 1D TEM models (Oldenburg and Li, 1999; Oldenborger et al., 2007).

RESULTS

S2007

Results for inversion of the three soundings along section S2007 are illustrated in Figure 2. From East to West, Site 2 represents a till target, Site 1 represents a buried valley target and Site 3 represents a bedrock target (Figure 1). Although the decay curves a relatively similar, the three target types are clearly distinguished in the apparent resistivity curves and the difference is manifest in the 1D resistivity models.

For Site 1, the incised buried valley is recovered as a large resistive anomaly of approximately 60 Ωm from 40–85 m depth indicative of coarse-grained material as observed at the bottom of borehole Kilcart#8 (Oldenborger et al., 2013). The variability between the L_1, L_2 and L_2 DOI models indicates that there is some uncertainty as to the absolute resistivity of the buried valley, but not so much as to render the anomaly unreliable. Above the buried valley, we interpret the till to be comprised of two electrically distinct units: approximately 17 Ωm from 0–

14 m depth, and 10–12 Ωm from 14–40 m depth. This heterogeneity in the till package is not observed in the AeroTEM resistivity models, but is supported by borehole and electrical resistivity data (Crow et al., 2012a; 2012b; Oldenborger et al., 2013). Beyond 85 m depth, the model predicts a resistivity of 3–6 Ωm which we interpret to represent shale bedrock. This bedrock resistivity is in agreement with borehole data (Crow et al., 2012a)

At Site 2, we observe a similar heterogeneous surficial till package, but also a moderate resistive anomaly above bedrock: approximately 40 Ωm from 40–65 m depth. Again, this feature is not obviously apparent in the AeroTEM results, but it does correlate to the adjacent electrical resistivity survey. The TEM and supporting data suggest that this moderately resistive basal layer is distinct from the incised buried valley fill. However, the exact relationship is unclear.

At Site 3, bedrock appears to occur at approximately 20 m depth with the overlying material having a resistivity of 13–16 Ωm which we interpret to represent an electrically homogeneous package of till, perhaps equivalent to the top layer observed at Sites 1 and 2.

S3

The 1D resistivity models for the four sites along section S3 are illustrated in Figure 3. Again, the incised buried valley (Site 1) is recovered as a large resistive anomaly with a resistivity of approximately 60 Ωm from 40–90 m depth and the till package appears to be comprised of two electrically distinct units: approximately 25 Ωm from 0–14 m depth, and 15 Ωm from 14–40 m depth. To the South (Site 3), the surficial layer is observed to be thicker and more resistive. This observation is corroborated by electrical resistivity data and is consistent with a regional resistive AeroTEM anomaly in the Killarney area (Oldenborger et al., 2013) that may be a result of a transition to gravel, or till with gravel at the surface. At Site 3, the basal unit is less resistive than the buried valley and bedrock is shallower (approximately 60 m depth).

Site 4 is located over a shallow valley observed by Oldenborger et al. (2014) and Pugin et al. (2014). The shallow valley is manifest as a strong resistive anomaly in the TEM data – the most resistive material observed: approximately 150–200 Ωm from 0–25 m depth. This feature represents a potential aquifer in itself, or a potential recharge/transport pathway should it intersect the deeper buried valley.

S2

Section S2 is located over the eastern incised valley observed in the AeroTEM results (Figure 1, Oldenborger et al., 2013). Results for inversion of the two soundings along S2 are illustrated in Figure 4. Most interestingly, the eastern valley has markedly different electrical resistivity structure compared to the western valley. Site 1 shows a moderately resistive surficial layer to 20 m depth underlain by a less resistive layer over conductive bedrock at approximately 120 m depth. Depth to bedrock supports the interpretation that this is indeed a bedrock valley, but the resistivity of the fill is indicative of till or non-aquifer material. The borehole GSCSW07 indicates that eastern valley fill is dominated by till at the Canada-US border with a small amount of basal sand and gravel (Crow et al., 2012). At S2, there is no indication in the TEM inversions of a basal sand and gravel, but a thin resistor at this depth would be difficult to resolve. Site 2 indicates a significant amount of moderately resistive material on the eastern flank of the valley. These observations are corroborated by the adjacent electrical resistivity survey (Oldenborger et al., 2013).

CONCLUSIONS

This Open File has reported on ground-based TEM data collected by the GSC for the Spiritwood valley aquifer as part of the Groundwater Geoscience Program of Natural Resources Canada. One-dimensional modelling and inversion of the data show marked variability in the data and the resistivity models between different geological settings. The TEM data and models largely support conclusions drawn from the integration of other various data types and demonstrate that the Spiritwood valley aquifer system can be resolved into several electrically distinct units that can be reasonably classified in terms of sediment types.

In particular, depth to bedrock is clearly resolved in the TEM models and the incised buried valley interpreted from the regional airborne survey is associated with a relatively strong resistive anomaly indicative of coarser grained material or a high-potential aquifer. Compared to Spiritwood AEM surveys, the ground-based TEM data exhibit superior near-surface resolution and enhanced discrimination of electrical resistivity with values that are in agreement with borehole and surface electrical resistivity data. The TEM data will be useful for quantitative verification and calibration airborne time-domain electromagnetic data both in terms of the decay curves (data space) and distinct geological structure such as depth to bedrock (model space).
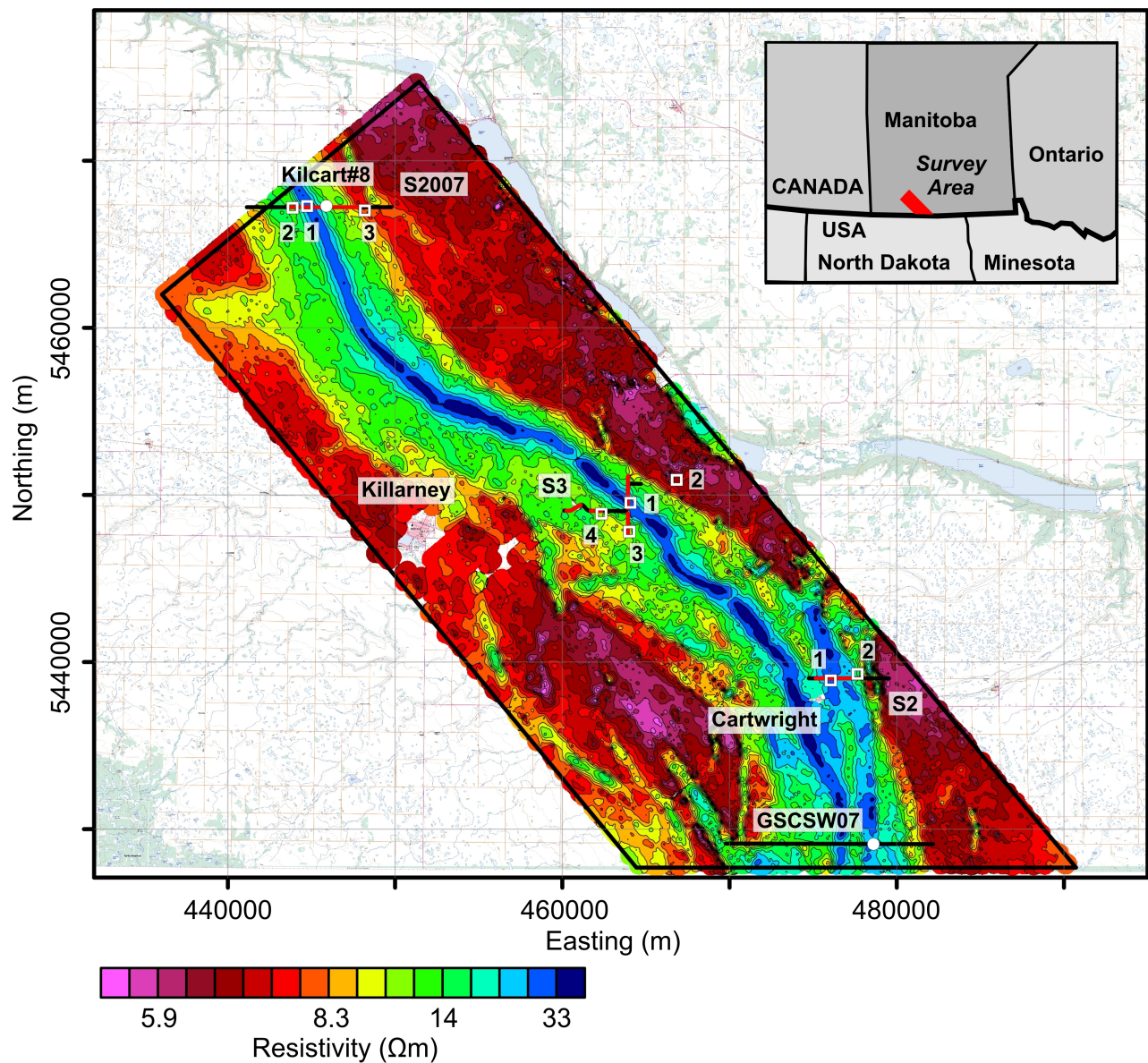
ACKNOWLEDGMENTS

FIGURES

Figure 1. Location map for TEM sounding sites (white squares) overlain on the electrical resistivity model from Sapia et al. (2014b) at an elevation of 395 masl (approximately 70 m depth). Also shown are existing seismic sections (black), electrical resistivity profiles (red) and the locations of boreholes Kilcart#8 and GSCSW07 (Crow et al., 2012).
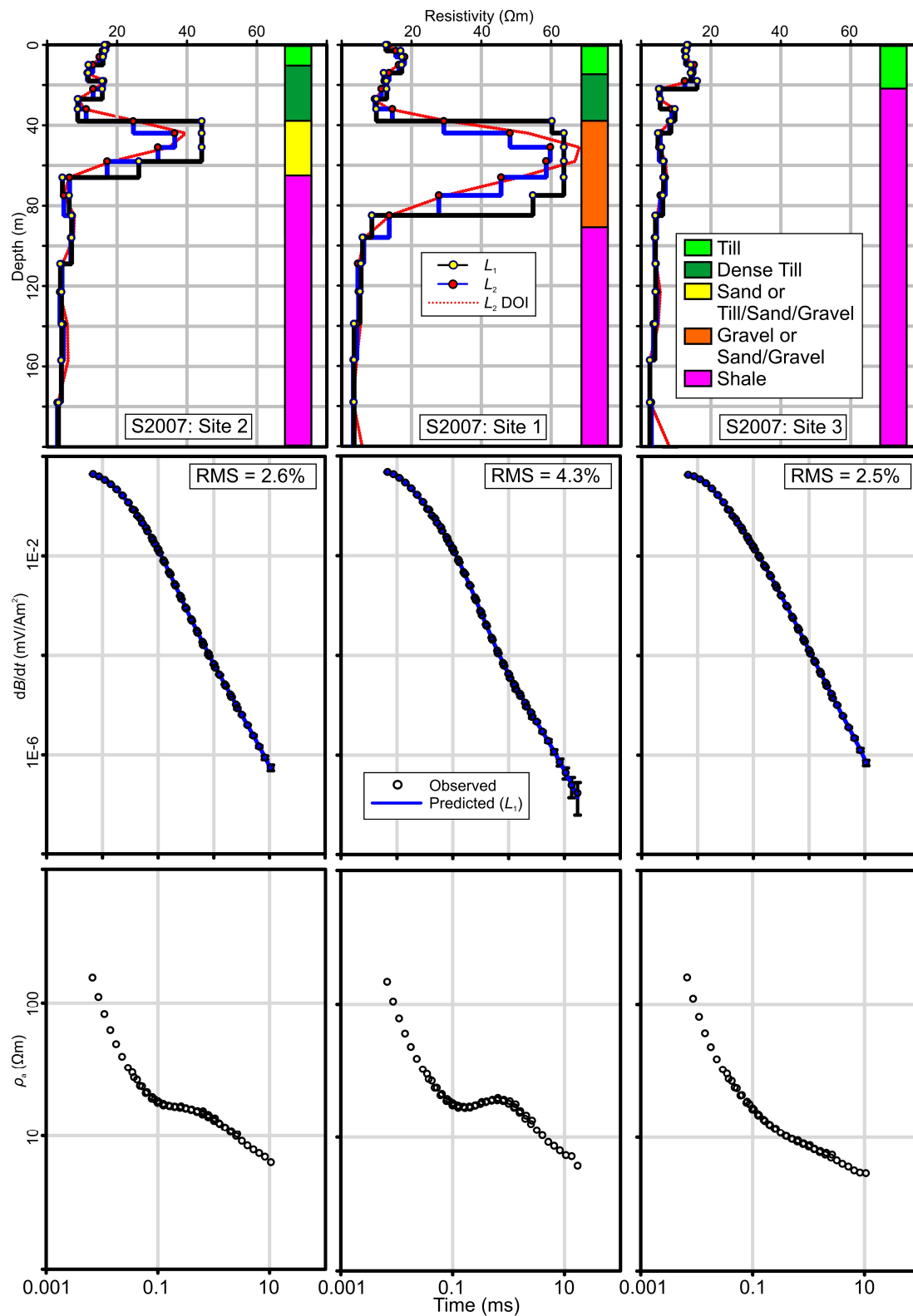
Figure 2. Data and inversion results for S2007. Top: 1D resistivity models from East to West. The color-coded pseudo-logs indicate electrically distinct units with a nominal classification scheme. Middle: observed and predicted decay curves. Bottom: apparent resistivity curves.
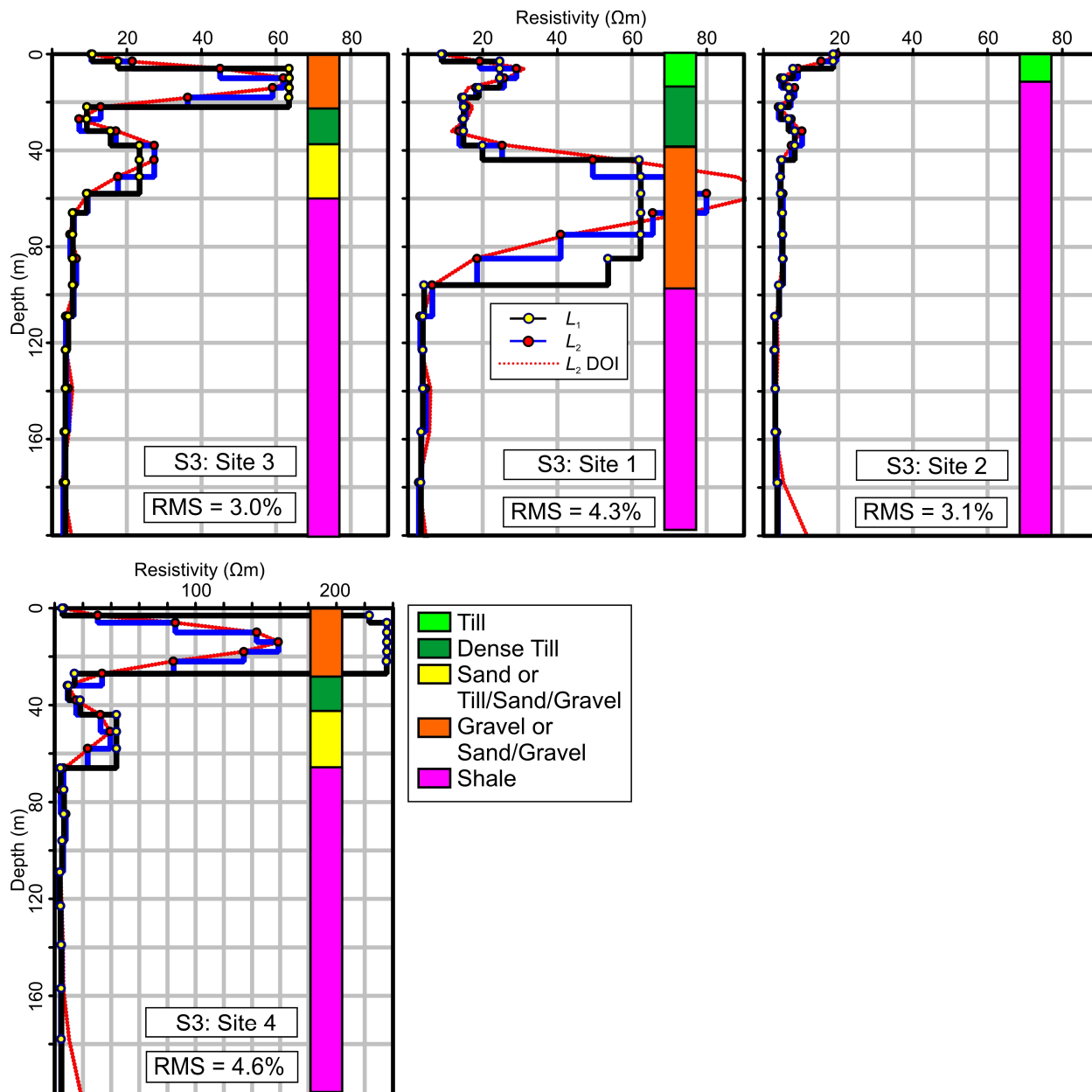
Figure 3. 1D resistivity models for S3. Top: sites from South to North. Bottom: shallow valley site. The color-coded pseudo-logs indicate electrically distinct units with a nominal classification scheme.
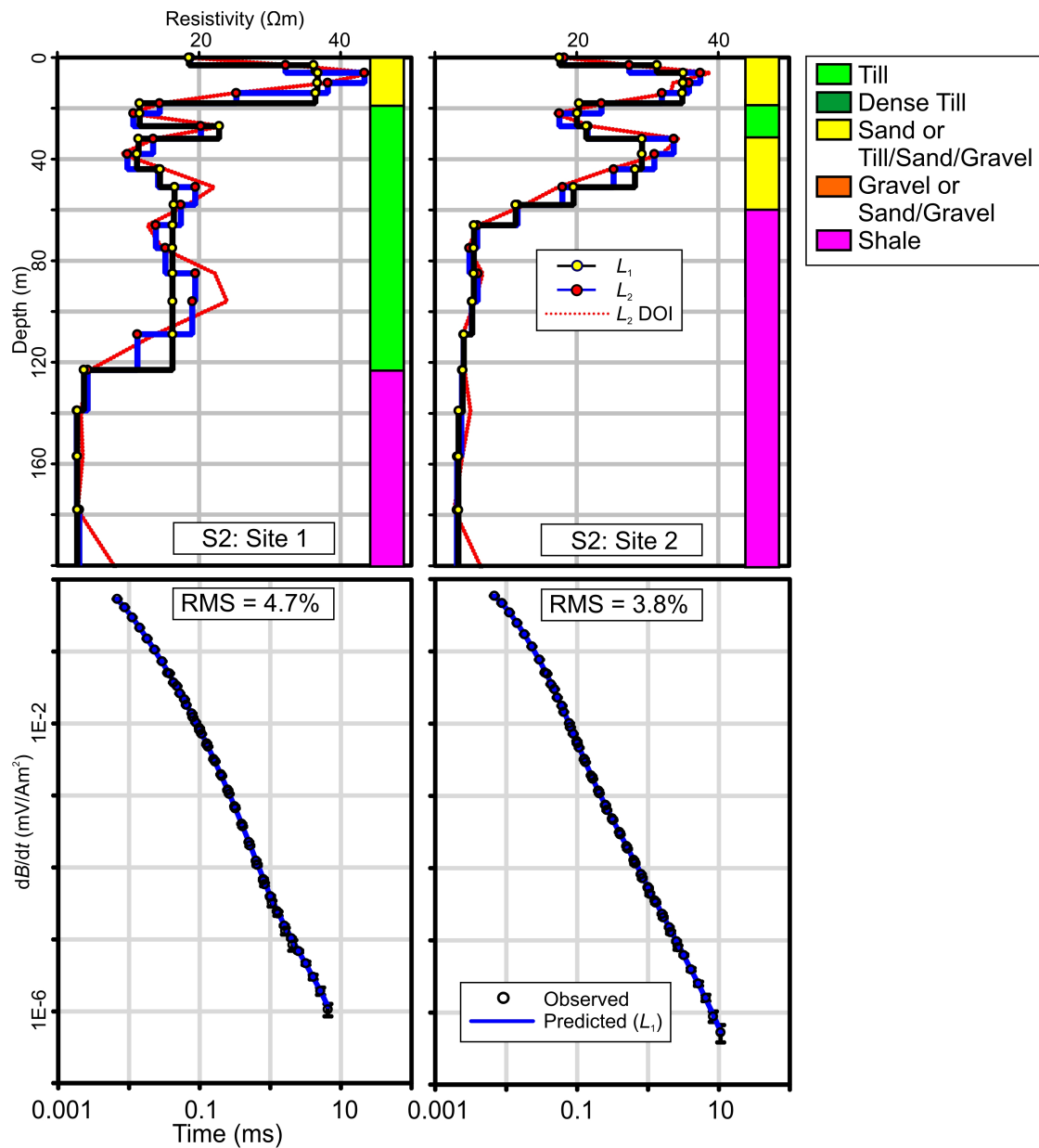
Figure 4. Data and inversion results for S2. Top: 1D resistivity models from East to West. The color-coded pseudo-logs indicate electrically distinct units with a nominal classification scheme. Bottom: observed and predicted decay curves.

REFERENCES

Betcher, R.N., Matille, G., Keller, G., 2005. Yes Virginia, there are buried valley aquifers in Manitoba. Proceedings of the 58th Canadian Geotechnical Conference, 6E-519.

Bluemle, J.P., 1984. Geology of Towner County, North Dakota. North Dakota State Water Commission, County Groundwater Studies 36, Part I.

Crow, H.L., Brewer, K.D., Pugin, A.J.-M., Russell, H.A.J., 2012a. Downhole geophysical data from boreholes along the Spiritwood buried valley aquifer near Cartwright, Killarney, and southeast of Brandon, Manitoba. Geological Survey of Canada, Open File 7080.

Crow, H.L., Knight, R.D., Medioli, B.E., Hinton, M.J., Plourde, A., Pugin, A.J.-M., Brewer, K.D., Russell, H.A.J., Sharpe, D.R., 2012b. Geological, hydrogeological, geophysical, and geochemistry data from a cored borehole in the Spiritwood buried valley, southwest Manitoba. Geological Survey of Canada, Open File 7079.

Danielsen, J.E., Auken, E., Jorgensen, F., Sondergaard, V., Sorensen, K.I., 2003. The application of the transient electromagnetic method in hydrogeophysical surveys. *Journal of Applied Geophysics* **53**, 181–198.

Farquharson, C.G., Oldenburg, D.W., 1993. Inversion of time-domain electromagnetic data for a horizontally layered Earth. *Geophysical Journal International* **114**, 433–442.

Farquharson, C.G., Oldenburg, D.W., 1998. Non-linear inversion using general measures of data misfit and model structure. *Geophysical Journal International* **134**, 213–227.

Foged, N., Auken, E., Christiansen, A.V., Sørensen, K.I., 2013. Test-site calibration and validation of airborne and ground-based TEM systems. *Geophysics* **78**, E95–E106.

Haber, E., Oldenburg, D.W., Shekhtman, R., 2007. Inversion of time domain three-dimensional electromagnetic data. *Geophysical Journal International* **171**, 550–564.

Legault, J.M., Prikhodko, A., Dodds, D.J., MacNae, J.C., Oldenborger, G.A., 2012. Results of recent VTEM helicopter system development testing over the Spiritwood Valley aquifer, Manitoba. Symposium on the Application of Geophysics to Environmental and Engineering Problems. Environmental and Engineering Geophysical Society, 114–130.

Oldenburg, D., Li, Y., 1999. Estimating depth of investigation in dc resistivity and IP surveys. *Geophysics* **64**, 403–416.

Oldenborger, G.A., 2010a. AeroTEM III Survey, Spiritwood Valley, Manitoba, parts of NTS 62G/3, 62G/4, Manitoba. Geological Survey of Canada, Open File 6663.

Oldenborger, G.A., 2010b. AeroTEM III Survey, Spiritwood Valley, Manitoba, parts of NTS 62G/3, 62G/4, 62G/5, 62G/6, Manitoba. Geological Survey of Canada, Open File 6664.

Oldenborger, G.A., Pugin, A.J.-M., Hinton, M.J., Pullan, S.E., Russell H.A.J., Sharpe D.R., 2010. Airborne time-domain electromagnetic data for mapping and characterization of the Spiritwood Valley aquifer, Manitoba, Canada. Geological Survey of Canada, Current Research 2010–11.

Oldenborger, G.A., Pugin A.J.-M., Pullan S.E., 2013a. Airborne time-domain electromagnetics, electrical resistivity and seismic reflection for regional three-dimensional mapping and characterization of the Spiritwood Valley Aquifer, Manitoba, Canada. *Near Surface Geophysics* **11**, 63–74.

Oldenborger, G.A., Routh, P.S., Knoll, M.D., 2007. Model reliability for 3D electrical resistivity tomography: Application of the volume of investigation index to a time-lapse monitoring experiment. *Geophysics* **72**, F167–F175.

Oldenborger, G.A., Sharpe, D.R., Pugin, A.J.-M., Russell, H.A.J., 2013b. Helicopter time-domain electromagnetic data over the Eastern Hatfield buried valley aquifer system, Saskatchewan, Canada. Geological Survey of Canada, Current Research 2013-13.

Podgorski, J.E., Auken, E., Schamper, C., Christiansen, A.V., Kalscheuer, T., Green, A.G., 2013. Processing and inversion of commercial helicopter time-domain electromagnetic data for environmental assessments and geologic and hydrologic mapping. *Geophysics* **78**, E149–E159.

Pugin, A.J.-M., Oldenborger, G.A., Cummings, D.I., Russell, H.A.J., Sharpe, D.R., 2014. Architecture of buried valleys in glaciated Canadian Prairie regions based on high resolution geophysical data. *Quaternary Science Reviews* **86**, 13–23.

Pugin, A.J., Oldenborger, G.A., Pullan S.E., 2011. Buried valley imaging using 3-C seismic reflection, electrical resistivity and AEM surveys. Symposium on the Application of Geophysics to Environmental and Engineering Problems. Environmental and Engineering Geophysical Society.

Randich P.G., Kuzniar, R.L., 1984. Geology of Towner County, North Dakota. North Dakota State Water Commission, County Groundwater Studies 36, Part III.

Russell, H.A.J., Hinton, M.J., van der Kamp G., Sharpe D., 2004. An overview of the architecture, sedimentology and hydrogeology of buried-valley aquifers in Canada. Proceedings of the 57th Canadian Geotechnical Conference, 26–33.

Sapia, V., Oldenborger, G., Viezzoli, A., 2012. Incorporating a-priori information into AEM inversion for geological and hydrogeological mapping of the Spiritwood Valley Aquifer, Manitoba, Canada. 31st National GNGTS Conference, Italy, 194–199.

Sapia, V., Oldenborger, G.A., Viezzoli, A., Marchetti M., 2014a. Incorporating ancillary data into the inversion of airborne time-domain electromagnetic data for hydrogeological applications. *Journal of Applied Geophysics* in press.

Sapia, V., Viezzoli, A., Jørgensen, F., Oldenborger, G.A., Marchetti, M., 2014b. The impact on geological and hydrogeological mapping results of moving from ground to Airborne TEM. *Journal of Environmental and Engineering Geophysics* in press.

Shaver R.B., Pusc, S.W., 1992. Hydraulic barriers in Pleistocene buried-valley aquifers. *Ground Water* **30**, 21–28.

Spies, B.R., Eggers, D.E., 1986. The use and misuse of apparent resistivity in electromagnetic methods. *Geophysics* **51**, 1462–1471.

van der Kamp, G., Maathius, H., 2012. The Unusual and large drawdown response of buried-valley aquifers to pumping. *Ground Water* **50**, 207–215.

Wiecek, S., 2009. Municipality of Killarney, Turtle Mountain groundwater assessment study. W.L. Gibbons & Associates Inc.

Winter, T.C., Benson, R.D., Engberg, R.A., Wiche, G.J., Emerson, D.G., Crosby, O.A., Miller J.E., 1984. Synopsis of ground-water and surface-water resources of North Dakota. United States Geological Survey, Open File Report 84-732.

APPENDIX

The Geonics ProTEM data used to generate the electrical resistivity models in this Open File are included as a Microsoft® Excel® spreadsheet (OF_7593_TEM_Data.xls). For each site, the data are provided as three separate integrated soundings of raw voltage for each base frequency along with three separate transmitter-off noise recordings for each base frequency, where acquired. Empirical noise models are fit to the ambient noise and repeatability errors for the raw data.

The edited and processed data and 1D electrical resistivity models for each site are included as a separate Microsoft® Excel® spreadsheet (OF_7593_TEM_Inversions.xls). The 1D resistivity models provided in this Open File are the result of iterative processing, editing and multiple inversions of the data. Only the final edits and processing are presented along with the final blocky and smooth models for each site. Additional information, including inversion parameter files, can be obtained by contacting the authors.